Radiation Protection Dosimetry, 2025, **201(5)**, 333–350
https://doi.org/10.1093/rpd/ncaf024
Advance access publication date 21 March 2025
Paper

OXFORD

Assessing nuclear energy and radiological risks: a case study of radionuclide dispersion from potential nuclear power plant accidents in Ghana

S. A. Birikorang[1,2,*], S. Dahunsi[3], S. Adu[1,2], C. A. Nketia[2], A. Blay[2,4]

[1]Nuclear Regulatory Authority, House 1&2, Neutron Avenue Ghana, P. O. Box AE 50 Kwabenya-Atomic Energy, Accra, Ghana
[2]Graduate School of Nuclear and Allied Sciences, University of Ghana, P. O. Box AE 1 Legon, Accra, Ghana
[3]Oak Ridge National Laboratory, 1 Bethel Valley Rd, Oak Ridge, TN 37830, United States
[4]Ghana Atomic Energy Commission, P. O. Box LG 80, Legon, Accra, Ghana

*Corresponding author. Nuclear Regulatory Authority, Ghana, P. O. Box AE 50 Atomic Energy, Accra, Ghana.
E-mail: sylvester.birikorang@gmail.com

Abstract

This study explored the significance of nuclear power and assessed radiological risks arising from potential containment leakage or failure, focusing on radionuclide dispersion and emergency preparedness. The findings revealed seasonal differences in radionuclide releases, with activities of 1.35×10^{15} Bq during the wet season and 4.70×10^{18} Bq in the dry season. Peak ground concentrations of ^{137}Cs in the wet season reached alarming levels of 6.22×10^{3} kBq/m^2 within 2.14 km of the release point due to deposition processes like rainout and washout. In contrast, the dry season showed ^{137}Cs ground concentrations of 4.88×10^{4} kBq/m^2, consisting primarily of noble gases. These results emphasize the importance of effective emergency preparedness strategies, including robust monitoring systems, evacuation plans, and public education. By focusing on protective measures informed by total effective dose equivalent assessments, this study highlights the need for proactive approaches to mitigate radiological hazards and enhance community resilience near nuclear facilities.

Introduction

Integrating nuclear energy into Ghana's energy mix represents a critical step toward achieving sustainable development and meeting the country's growing energy demands. However, adopting nuclear power comes with unique challenges, particularly the need for a robust emergency preparedness and response (EPR) framework to mitigate potential radiological risks. Nuclear energy development requires careful planning to ensure public safety, environmental protection, and regulatory compliance, focusing on addressing both anticipated and unanticipated emergencies. In line with this, Ghana must establish comprehensive EPR systems that align with international standards and best practices.

The International Atomic Energy Agency (IAEA) highlights the importance of implementing effective EPR frameworks as outlined in its General Safety Requirements (GSR Part 7). These standards provide a structured approach for countries to prepare for, respond to, and recover from radiological or nuclear emergencies [1]. Furthermore, the US Environmental Protection Agency's (EPA) Protective Action Guidelines (PAGs) serve as a critical tool in guiding emergency responses, particularly in determining protective actions to safeguard public health during incidents involving radiation exposure [2]. These international guidelines provide the foundation for developing national strategies that enhance readiness, build capacity, and prevent potential impacts. Ghana's commitment to nuclear energy was reinforced with the declaration of Phase 2 of the Nuclear Power Program in 2022, signifying the readiness of the country to advance its nuclear agenda [3]. Having a national EPR framework rooted in the principles of the IAEA and EPA is critical for managing radiological emergencies and fostering public confidence in nuclear energy as a safe and viable solution for Ghana's energy challenges.

This paper explores the role of EPR in Ghana's nuclear accident or emergency while integrating IAEA

Received: November 15, 2024. **Revised:** January 24, 2025. **Editorial decision:** February 26, 2025. **Accepted:** March 3, 2025

safety standards and EPA PAGs into national policies. It highlights the need for institutional collaboration, resource mobilization, and public engagement to ensure the effective implementation of EPR systems. By addressing these key areas, Ghana can enhance its nuclear security infrastructure and support the safe deployment of nuclear energy to meet its socioeconomic and environmental goals.

Potential radiological risk

People are becoming more aware of the potential radiological effects of nuclear accidents, and assessing these incidents plays a key role in building public trust and confidence. Under normal conditions, nuclear power plants (NPPs) do not release significant levels of radioactivity into the atmosphere. However, accidents, sabotage, or attacks can pose serious risks to public safety and the environment. This has been seen in incidents like Fukushima in 2011 [4], Chernobyl in 1986 [5], and Three-Mile Island in 1979, as well as other radiological events [6]. Such incidents are often triggered by natural disasters, human errors, or equipment failures, resulting in the release of harmful radiation. Ensuring nuclear safety is vital for the operation of nuclear reactors [7]. Nuclear reactor safety depends on three key defensive barriers. The first is the fuel cladding, which encases the nuclear fuel and prevents radioactive substances from escaping. The second barrier, the primary circuit, ensures that radioactive materials do not enter the reactor coolant. The third is the containment system, which acts as a final shield, preventing radioactive materials from escaping into the environment in case of a reactor vessel breach. A loss-of-coolant accident (LOCA) compromises the second barrier, leading to cascading challenges for the other two. When the primary circuit fails, the fuel cladding is exposed to intense heat from the decaying fuel without the cooling effect of the circulating coolant [8, 9]. Simultaneously, the containment system comes under severe pressure from the escaping reactor coolant, heightening the risk of failure. These conditions underscore the severity of LOCA scenarios and their implications for nuclear safety. A LOCA is a theoretical incident where the coolant in a nuclear reactor is rendered inaccessible due to a rupture in the primary coolant pipes or a malfunction in the reactor's cooling systems. This situation can result in a loss of cooling efficiency, causing a sharp increase in fuel temperature, which may lead to fuel damage and the possible release of radioactive substances [10].

The accident scenario in this study focused on security-related events—particularly terrorist attacks on NPPs—but was limited to security implications. This approach will help determine the dose effects and inform emergency decision-making during severe accidents, thus emphasizing the need for comprehensive and more robust emergency response strategies. In the study, a LOCA event is initiated by the explosion of a critical component, the power supply resulting in the damage of the cold leg pump, which connects the In-containment Refueling Water Storage Tank (IRWST) to the reactor vessel. This failure reduces the primary coolant supply, disrupting the cooling system and compromising the reactor's defensive barriers. These examples highlight the complexity of LOCA scenarios and the need for stringent safety measures to address such risks effectively. The LOCA scenario was chosen over other potential scenarios because it is widely used as a benchmark in international nuclear safety standards. As it has been cited in the IAEA's safety reports, global nuclear risk assessments and regulatory frameworks commonly focus on LOCA scenarios. [11]. Selecting this scenario ensures that Ghana's assessment aligns with global practices, supporting compliance and encouraging collaboration with international stakeholders. Due to the low fuel enrichment, a nuclear explosion is impossible in reactors. Instead, the most severe accident that could occur is a major LOCA, which can initiate a core meltdown [12]. Therefore, LOCA is considered a worst-case scenario.

A radiological assessment is essential to the Environmental Impact Assessment (EIA) process. Nuclear scientists in the country have stated in research articles the importance of assessing potential nuclear accidents using hypothetical scenarios and defining appropriate emergency response plans for nuclear facilities, which are crucial in evaluating the likelihood of incidents and their consequences [13–15]. This assessment helps identify and address potential radiation risks to people and the environment, ensuring safety and minimizing harm. The threat of nuclear leading to radiological consequences has become a pressing global issue. The public has a perceived notion that the country lacks comprehensive EPR strategies for potential radiological incidents; thus, the decision to deploy nuclear energy as part of Ghana's energy mix would be a major issue to consider. The present article highlights the significance of analyzing Ghana's preparedness for radiological emergencies by analyzing radionuclide dispersion scenarios resulting from potential NPP accidents. This study assessed whether the country has effective EPR strategies to ascertain the validity of the public perception.

This work focuses on the Hualong Pressurized Reactor 1000 (HPR1000), a nuclear reactor developed by the China General Nuclear Power Group, as its case study. Ghana is working with "China National Nuclear Corporation Overseas Limited" under an agreement to collaborate on the development of a NPP [16]. This

Table 1. Key features of HPR1000 NPP.

Parameter	Value
Core thermal power	1100 MW
Design pressure	17.23 MPa (abs)
Average fuel burnup	60 000 MWD/MTU
Design leak rate	0.1% per day
Number of fuel assemblies	177 (12 ft)
Steam generator water mass	315 000 kg
Containment volume	70 000 m^3
Coolant mass	3.185×10^5 kg
Discharge burnup in spent fuel storage	50 000 MWD/MTU
Steam generator steaming rate	5688 000 kg/h
Bypass flow rate	4000 kg/h

work employed the Radiological Assessment System for Consequence Analysis (RASCAL) 4.3.4 code for the dose assessments, which is a computer code designed for emergency response planning and radionuclide dose assessment [17]. The consequences of nuclear accidents have sparked significant debate, resulting in extensive research aimed at understanding their aftermath. In the design and simulation of reactor accident analyzes, considerable emphasis was placed on the reactor core. Damage or degradation of the reactor core can initiate various types of accidents, including reactivity excursions, increased core temperature, and loss of primary coolant. Many of these accidents are often primarily caused by straightforward human errors, which can occasionally involve intentional sabotage or attacks on the facility [18].

The proposed HPR1000 reactor

The HPR1000 (Hualong One) is a commercial NPP and one of the most advanced power plants with significant features, including both active and passive safety designs, making it highly resistant to accidents. Table 1 describes the key technical features of the plant, which are also used in the simulation code for the accident analysis. Many newcomer countries are choosing the HPR1000 because of its advanced features, efficiency, and role in reducing carbon emissions, contributing to global efforts in carbon emission reduction.

Description of atmospheric dispersion simulation code

This work used RASCAL 4.3.4, a tool developed by the US Nuclear Regulatory Commission for independent dose projections during radiological emergencies. The choice of computational model is key to making accurate assessments. RASCAL employs Gaussian distribution methods to estimate how radionuclides are released and how many individuals close to nuclear facilities may be exposed to radiation. The code includes various models that predict the release of radionuclides over time, how they spread in the environment, and the potential consequences. It simplifies reactors as basic structures linked by pathways, allowing the tool to estimate which radioactive materials are released and how they move through the environment. The system also integrates real-time weather data to enhance its predictions of how radiation is transported, dispersed, and deposited in the atmosphere. RASCAL 4.3.4 uses two different models to improve accuracy—a Gaussian plume model for short-range transport and a Lagrangian Gaussian puff model for long-range transport—making it more useful to researchers. It calculates radiation doses from different exposure pathways, including submersion, inhalation, and ground shine, although it does not estimate ingestion doses. It offers a general sense of which radionuclides are most critical when ingestion poses a potential risk. Compared with other atmospheric dispersion tools, RASCAL's real-time weather data and dual plume/puff models give it an advantage, allowing for more precise and flexible projections, especially during complex emergencies [17].

Theory of the dispersion mode

The RASCAL 4.3.4 code is a tool used by the Protective Measures Team in the US Nuclear Regulatory Commission's Operations Center. The code is used for making independent dose and consequence projections during radiological incidents and emergencies. The code was developed as a tool for the rapid assessment of an incident or accident at a US Nuclear Regulatory Commission-licensed facility and aids decision-making, such as whether the public should evacuate or shelter in place. The code is a first-order approximation of the radiation effects associated with the atmospheric release of radioactive materials. The mathematical expression employed in the Gaussian plume model is shown in Equation (1).

$$\chi\left(x,y,z\right) = \frac{Q}{2\pi\sigma_y\sigma_z}\exp\left[-\frac{1}{2}\left(\frac{y}{\sigma_z}\right)^2\right]x \left\{\exp\left[-\frac{1}{2}\left(\frac{z-H}{\sigma_z}\right)^2\right]+\exp\left[-\frac{1}{2}\left(\frac{z+H}{\sigma_z}\right)^2\right]\right\}. \quad (1)$$

In Equation (1), H is the height of the plume (m); σ_y and σ_z are the horizontal and vertical deviations of plume concentration distribution, respectively (m); Q is the uniform emission rate of pollutants (kg/s); x is the long wind coordinate measured in wind direction from the source (m); y is the crosswind coordinates direction (m); z is the vertical coordinate measured from the ground (m), χ (x, y, z) is the mean concentration of diffusing substance at a point (x, y, z) (kg/m3); and μ is the mean wind velocity affecting the plume along the x-axis (m/s).

The maximum concentration occurs when,

$$\sigma_z = \frac{H}{\sqrt{2}}. \quad (2)$$

At large distances from the source, where σ_z is much larger than H, the concentration varies in proportion to $\frac{1}{(\sigma_y.\sigma_z)}$.

If the initial momentum of the plume dominates, then an approximate expression for the final plume rise is

$$\Delta h = \frac{3DW}{U}, \quad (3)$$

where D is the diameter of the source, W is the stack exit diameter (m), and U is the initial vertical velocity of the plume (m/s).

The formula for the stable case is

$$\Delta h = 2.4\left(\frac{F_b}{us_p}\right)^{1/3}. \quad (4)$$

where Δh is the change in height or the vertical dispersion of the material being released (m) and reflects how high the material travels in the atmosphere. F_b isthe buoyancy flux, which is a measure of the upward force exerted by materials released into the atmosphere. u_s isthe wind speed at the surface (m/s) and p is the atmospheric pressure at the location where the release occurs (Pa).

In the case in which the weather is unstable [Equation (5)) or neutral (Equation (6)], Briggs deduced that

$$\Delta h = 4.3\left(\frac{F_b}{uw_*^2}\right)^{3/5} z_i^{2/5}, \text{and} \quad (5)$$

$$\Delta h = 1.54\left(\frac{F_b}{uu_*^2}\right)^{3/5} z_i^{1/3}. \quad (6)$$

In Equations 5 and 6 uw_* is the wind speed at the ground or near the source, a parameter that defines the horizontal wind speed that influences the dispersion of the plume. z_i is the vertical mixing height of the atmospheric boundary layer which defines the height at which air becomes well-mixed with radionuclides.

When there is a choice between a breakup formula and a Briggs formula, the one giving the minimal plume rise is chosen.

Lucas *et al.* [19], developed a formula for unstable and neutral atmospheric conditions as,

$$\Delta h = \left(\frac{60+5H}{u}\right) \text{x } Q_{\mathrm{H}}^{0.25}. \quad (7)$$

For average meteorological conditions,

$$\Delta h = \left(\frac{275+2H}{u}\right) \text{x } Q_{\mathrm{H}}^{0.25}, \quad (8)$$

where H is the physical stack height and Q_H is the heat emission from a stack (k cal/s).

The plume rise formula was originally developed by Holland [20] and was applied to all stability conditions. The formula was later modified by Stümke *et al.* [21]:

$$\Delta h = \frac{V_s d}{u}\left[1.5 + 2.68 \times 10^{13} p\left(\frac{T_s - T_a}{T_a}\right) d\right], \quad (9)$$

where Δh is the plume rise (m), V_s is the stack exit velocity (m/s), D is the internal stack diameter (m), u is wind speed (m/s), p is atmospheric pressure (hPa), T_s is the stack gas temperature (K), T_a is the air temperature (K), and A is a coefficient dependent on stability.

The "Gaussian plume model" (Fig. 1) incorporated in the RASCAL 4.3.4 code helped predict how pollutants, such as radionuclides, spread through the air after being released.

This ability is especially useful in planning radiological emergencies. It allows authorities to understand where and how far contaminants might travel, helping responders take appropriate action to protect people and the environment.

The "Gaussian plume model" incorporated in the RASCAL 4.3.4 code helps to predict how pollutants, like radionuclides, spread through the air after being released, as shown in Fig. 1. This is especially useful in planning radiological emergencies. The model is a tool that uses mathematical simulations to understand how pollutants move, spread, and change in the atmosphere. It helps estimate the concentration of air pollution downwind, using data about pollutant emissions and the characteristics of the atmosphere. It allows authorities to understand where and how far contaminants might travel, helping them take appropriate action to protect people and the environment [23].

Model assumptions

The following model assumptions were considered during the simulation process:

(1) The model is considered accurate for downwind distances between 100 and 2000 m.

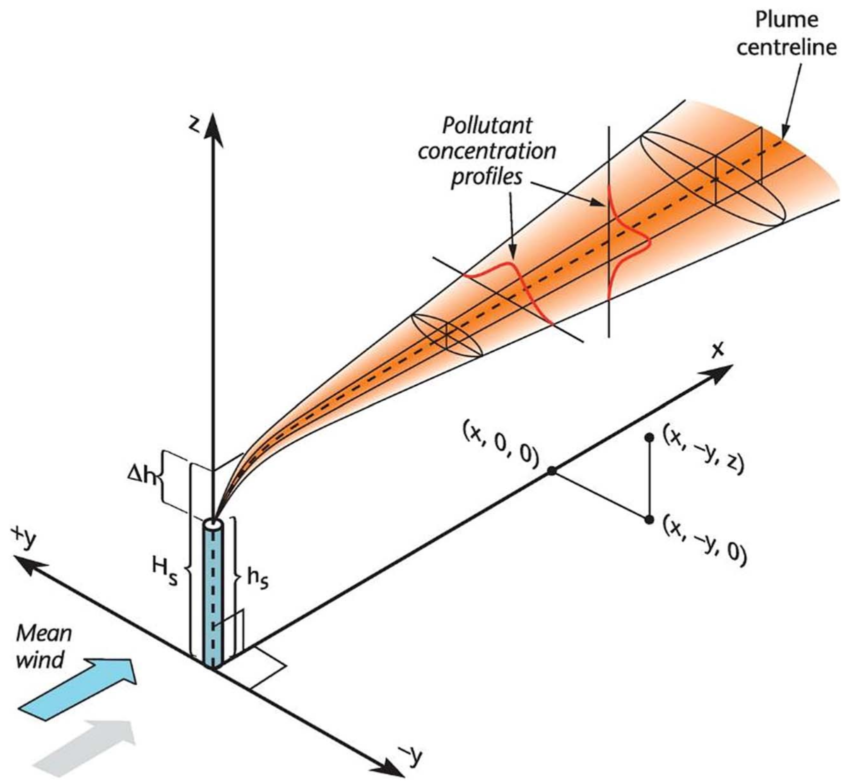

Figure 1. Geometry of a Gaussian plume [22].

(2) For shorter distances, the model assumes a steady and smooth wind flow moving directly away from the release source, without any disturbances or changes in direction.
(3) For distances over 2000 m, the model accounted for the local terrain and weather conditions.
(4) It assumes that the pollutants released into the air do not react chemically as they move through the atmosphere.

Model limitations

During the simulation process, we considered certain limitations of the model to address potential challenges and reduce the risk of bias.

(1) The dispersion coefficients (σ_y and σ_z) used in the model might not be highly accurate.
(2) The model neglects the turning of wind due to frictional effects, which can cause the plume to spread in the crosswind direction.
(3) The model does not account for ground deposition of concentrations that are negligible in value thus, below the detection threshold upon reaching the ground.

Materials and methods

Site meteorological data

The meteorological data as presented in Tables 2 and 3 for the site location were obtained from the Ghana Meteorological Agency and cover a 5-year period from 2018 to 2023. The climate of Ghana is tropical and has two main seasons: wet (April to mid-October) and dry (mid-November to April). Ghana experiences two peaks in rainfall from May through June, September, and October. During these times, the weather is influenced by warm, moist southwest monsoon winds. Conversely, the dry season, Harmattan, occurs in December and January and is characterized by minimal rainfall. The data collected from this time period include average wind speed, wind direction, temperature, and relative humidity. These parameters were then entered into the meteorological data section of the RASCAL code for the analysis, as required. Measurements were taken from a meteorological instrument positioned at a height of 1.5 m. The tower provided measurements at multiple heights above sea level. The tower offered data at higher altitudes, eliminating the need for extrapolation.

The dry season pattern is characterized by low humidity, high temperatures, and strong winds. These conditions can significantly affect the dispersion of

Table 2. Site meteorological data for dry season.

Year	Temperature (°C)		Relative humidity	Winds speed (m/s)	Direction (°)
	Max.	Min.			
2018	29.533	23.233	80.43	5.75	193.333
2019	31.467	23.417	76.30	5.07	183.333
2020	29.900	23.983	81.88	6.70	288.333
2021	31.167	24.500	80.37	5.92	178.333
2023	30.527	23.523	78.77	7.02	172.667
Yearly Mean	30.518	23.731	79.55	6.09	203.199

Table 3. Site metrological data for wet season.

Year	Temperature (°C)		Relative humidity	Winds speed (m/s)	Direction (°)
	Max.	Min.			
2018	26.163	21.101	60.73	3.03	148.337
2019	27.712	23.332	62.90	2.80	153.232
2020	30.123	22.503	59.88	2.75	168.431
2021	29.616	24.403	63.25	3.07	171.667
2022	28.373	23.180	62.57	2.15	156.667
Yearly Mean	28.397	22.904	61.86	2.81	159.667

radioactive plumes in the event of a radiological release. At higher temperatures, convection currents increase as air masses rise, which affects the dispersion pattern of released radionuclides and leads to a higher dispersion rate.

For example, lower humidity means less moisture exists in the air to absorb the radionuclides, allowing them to travel farther distances. Strong winds are typical during the dry season in Ghana, and they play a crucial role in the dispersion of particles during a release. These patterns are essential for understanding their effect on radionuclide dispersion. Figures 2 and 3 illustrate the climate chart for Axim and the wind pattern, indicating that the predominant wind direction is from the southeast. Therefore, conditions for the dry season are vital for emergency planning regarding particle dispersion, making accuracy in modeling essential. Tables 2 and 3 present the site meteorological data from December to April 2018 through 2023 (i.e. dry season) and the wet seasons.

Windrose provides an easy-to-read visual overview of how often the wind blows in different directions and at various speeds over time at the site. This helps readers understand the local wind patterns, which is essential for assessing environmental impact, planning emissions control, and ensuring safety.

This wind rose provides a visualized summary of wind speed and direction frequencies over a specific period at the site. The plot highlights the predominant wind directions and their associated speeds for understanding local atmospheric conditions. This information is important for assessing potential environmental impacts, planning for emissions control, and ensuring safety at the site. Table 4 shows the average wind speeds and the associated atmospheric stability classes (refers to how well the air mass surrounding the stack is encouraged not to move up or down) used in the dispersion model. The study site at Axim is located along the coastline in the Ahanta West District of the Western Region of Ghana, situated at an elevation of 38 m, as shown in Fig. 4.

Proposed hypothetical accident scenario

In the hypothetical scenario in this study, an armed drone flew into the reactor building, targeting vital systems such as the cooling infrastructure and backup generators. It carried small explosives designed to disable these critical systems. When the explosives detonated, causing a devastating station blackout by destroying the backup generators. This blackout leads to a chain reaction of failures, including the disruption of the reactor's water supply due to the malfunction of the cold leg pump (see Fig. 5).

As the cooling system fails, the reactor core begins to overheat—a defining feature of an LOCA. Without

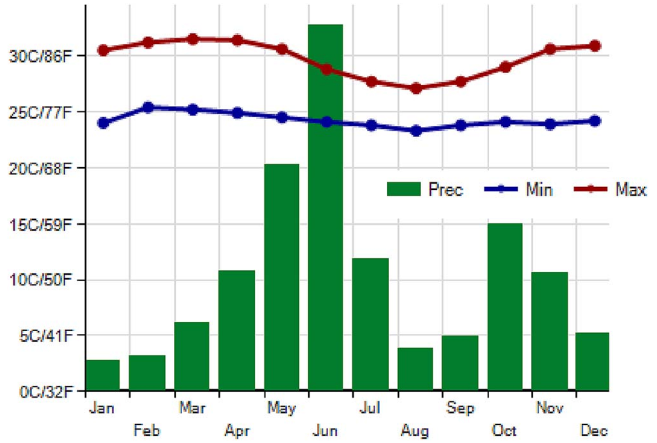

Figure 2. Climate pattern in Axim.

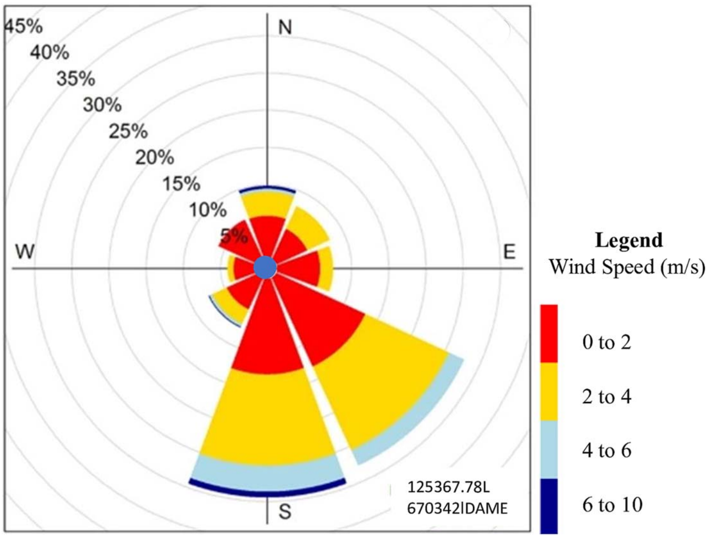

Figure 3. Windrose pattern showing predominant southeast direction for dry season.

sufficient coolant flow, the heat generated by the decaying fuel surpasses safe levels, resulting in the partial meltdown of ~20% of the reactor's fuel. This partial meltdown significantly threatens the integrity of the reactor's protective barriers (the third barrier), raising the risk of radioactive material being released into the environment. Fortunately, recovery teams manage to regain control before the situation worsens. Although the containment systems are pushed to their limits, they successfully prevent the meltdown from escalating into a catastrophic event or causing widespread contamination. This incident highlights the urgent need for stringent security measures to protect nuclear facilities from intentional attacks. It also underscores the importance of robust emergency preparedness, including plans for rapid response to mitigate the consequences of such high-risk scenarios. Figure 6 shows the Event Tree diagram of the attack. It traces the sequence of events starting from the attack and branches out based on potential outcomes at each stage.

The consequences of the attack:

(a) The drone attack damaged the cooling systems, causing a prolonged loss of coolant flow to the reactor core.
(b) The heat generated due to the malfunctioning pump connecting the IRWST caused the cladding to crack or rupture.
(c) The heat from the damaged reactor caused hydrogen gas to build up in the containment area because of the chemical reaction between the zirconium cladding and water.

Table 4. Wind speed and stability classes used in the dispersion model.

Season	Average wind speed (m/s)	Stability class	Assumption
Wet	2.81	D	Condition: (i) Neutral atmospheric condition (ii) Cloudy with moderate wind speed (iii) Less adiabatic cooling Reason: Because of cloud cover and mild weather during the rainy season in Axim
Dry	6.09	B	Condition: (i) Moderately unstable atmospheric condition (ii) No cloud cover and with no change (iii) Vertical mixing in the air and moderate wind speed (iv) Adiabatic cooling Reason: No cloud cover and vertical mixing causes a high rate of dispersion

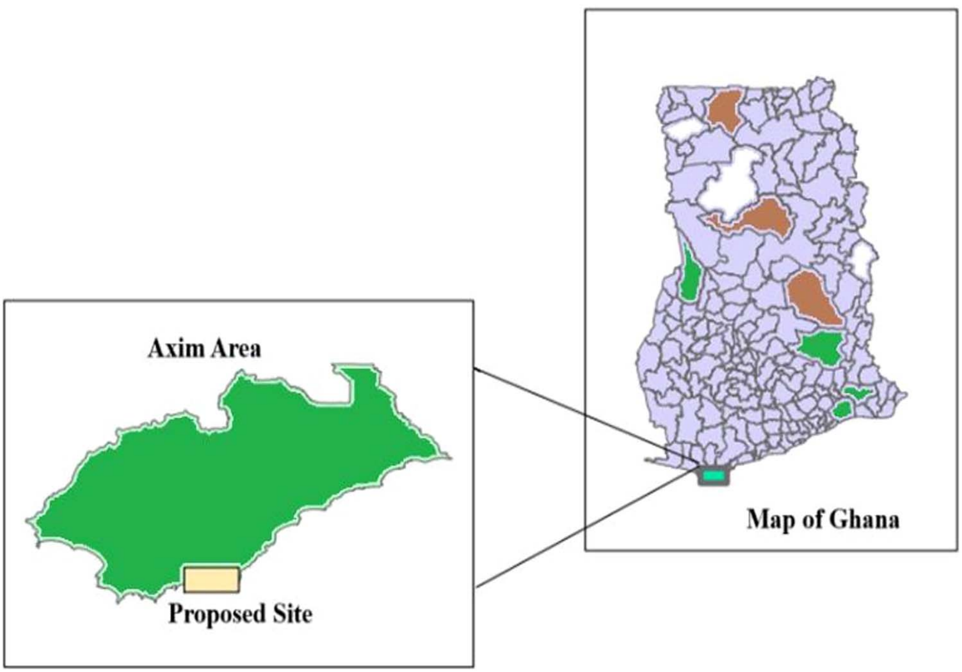

Figure 4. Research study site for the proposed reactor.

(d) High pressure built up in the reactor vessel because of the overheating, with malfunctioning safety relief valves.
(e) The attack delayed the deployment of external emergency response teams, prolonging the reactor recovery time.
(f) The attack disabled the emergency venting systems, which are crucial for controlling pressure and preventing the reactor from overheating.

A technical assumption for the accident scenario

(a) The reactor was operating at 1100 MWe before the accident.
(b) The release rate of radionuclides was 0.2 vol% per day, with a release height of 52.2 m.
(c) Reactor shutdown, core uncovering, and core recovery times were at 09:00, 11:00, and 13:00, respectively, for both wet and dry seasons.

The RASCAL 4.3.4 code identifies three possible release pathways for radionuclides: containment bypass, steam generator tube rupture, and containment

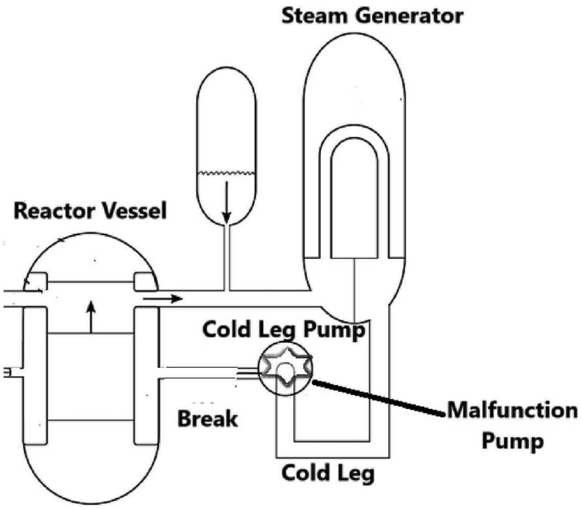

Figure 5. Schematic diagram showing the exact location of the break [24].

leakage or failure. In this study, the focus was on containment leakage or failure as the release pathway. During the LOCA event, a malfunction in the cold leg pump led to a loss of coolant, causing the reactor core to overheat. This overheating resulted in the partial meltdown of the fuel rods, generating high-pressure conditions within the containment. The subsequent containment failure allowed radionuclides to escape into the atmosphere.

Code simulation procedure

The simulation was initiated by selecting the primary tool, the Source Term to Dose tool, followed by feeding the code with the information required for reactor parameters, accident scenarios, and meteorological conditions. Figure 7 shows the simulation process for the RASCAL 4.3.4 code. The pathway selected for the accident scenario was the containment leakage or failure for wet- and dry-season scenarios.

The study's findings highlight a clear difference in radionuclide releases between the wet and dry seasons in the event of an NPP accident after the simulation. Table 5 provides a summary of the activity levels of the released radionuclides. This information is crucial for evaluating the radiological effects and understanding how effective safety and containment measures are in potential release situations.

These seasonal variations suggest that radionuclide dispersion could affect emergency preparedness in many ways. The high levels of noble gases in the dry season indicate a greater risk of rapid radionuclide spread because no precipitation is present to limit dispersion, complicating the emergency response. In contrast, iodine's presence in the wet season raises concerns for potential water and soil contamination, which could affect the local environment and public health in the long term. These results emphasize the need for adaptable emergency response strategies for immediate dispersion risks and environmental contamination that should be based on seasonal factors.

Results and discussion

This study evaluated postulated hypothetical accident scenarios resulting in core damage and release of radionuclides because of containment leakage or failure. Scenarios included the wet season and dry season. Radiological doses, including total effective dose equivalent (TEDE), thyroid effective dose equivalent and doses for the three exposure pathways—inhalation, cloud shine and ground shine—were estimated for each scenario. A comparison of the variation of TEDE with wind speed for the dry (stability class B) and wet (stability class D) seasons under the containment leakage or failure release pathway using the three selected stability classes as presented in Figs 8 and 9. The analysis of TEDE was important for the recommended protective actions.

The research compared how the TEDE changes with wind speed during the wet and dry seasons for the containment leakage scenario, using three different stability classes considering the minimum, average and maximum wind speed, as shown in Figs 8 and 9. Analyzing the TEDE is crucial for determining the recommended protective actions in response to these potential accidents. As horizontal transport increased, TEDE values rose at moderate wind speeds under stability class D in the wet and dry seasons. This increase kept the plume concentrated at downwind locations because of limited vertical mixing which kept the plume of released radionuclides concentrated at downwind locations. This situation heightens the risk of exposure for nearby populations. Research indicates that stable atmospheric conditions, like those found in stability class D, can significantly affect how airborne contaminants spread, resulting in higher localized doses [25]. This underscores the necessity of understanding atmospheric stability when evaluating potential health risks associated with nuclear incidents. When we compare these findings to other studies, a clear trend emerges increased horizontal transport during stable conditions often correlates with higher radiological doses in certain areas. This emphasizes the importance of effective monitoring and protective strategies to safeguard communities that may be exposed during such events [26].

Figures 10 and 11 show the relationship between TEDE and distance from the release point at different

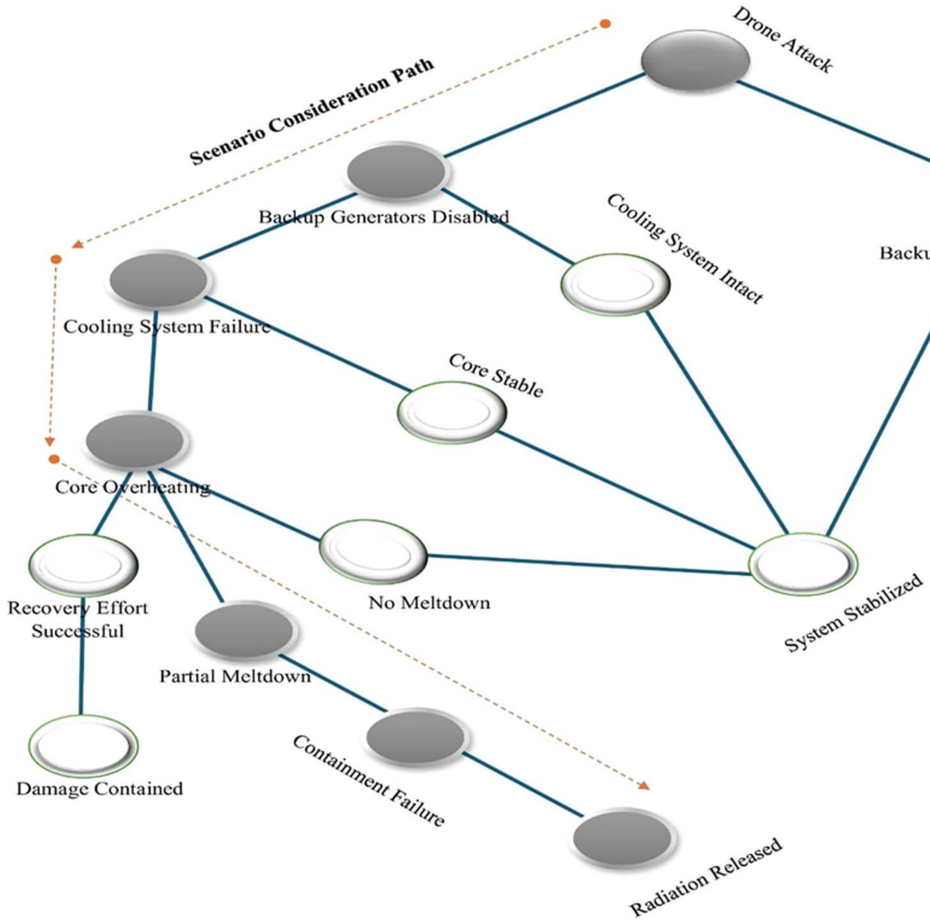

Figure 6. Schematic flow diagram illustrating the event tree for the drone attack.

Table 5. Summary of activity of released radionuclides.

	Containment leakage/failure: wet season		Containment leakage/Failure: dry season	
Radionuclides	Activity (Bq)	Total percentage (%)	Activity (Bq)	Total percentage (%)
Noble Gas	9.50×10^{14}	70.5	4.70×10^{18}	100
Iodine	3.10×10^{14}	22.7	2.41×10^{-11}	0
Other	9.20×10^{13}	6.8	1.20×10^{-12}	0
Total	1.35×10^{15}	100	4.70×10^{18}	100

stability classes during the dry and wet seasons for the containment leakage or failure release pathway.

The variation of TEDE with distance from a release point in dry and wet seasons which were analyzed under stability classes B (slightly unstable) and D (neutral) respectively reveals key differences in how radiation spreads based on seasonal and atmospheric conditions.

Under stability class D, the lack of vertical mixing keeps the plume more concentrated near the release site, resulting in higher TEDE levels close to the source. This can pose a significant exposure risk, particularly during dry conditions when radionuclides stay airborne longer [9]. Studies confirm that neutral or stable atmospheric conditions often lead to concentrated radiation exposure downwind from a release, which requires

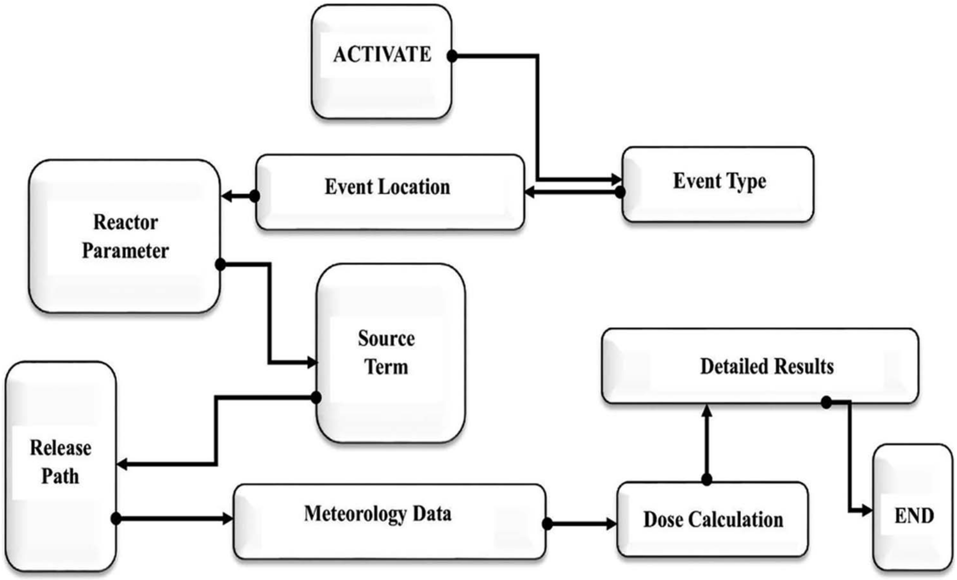

Figure 7. A flowchart illustrating the input procedure for the RASCAL 4.3.4 code simulation process.

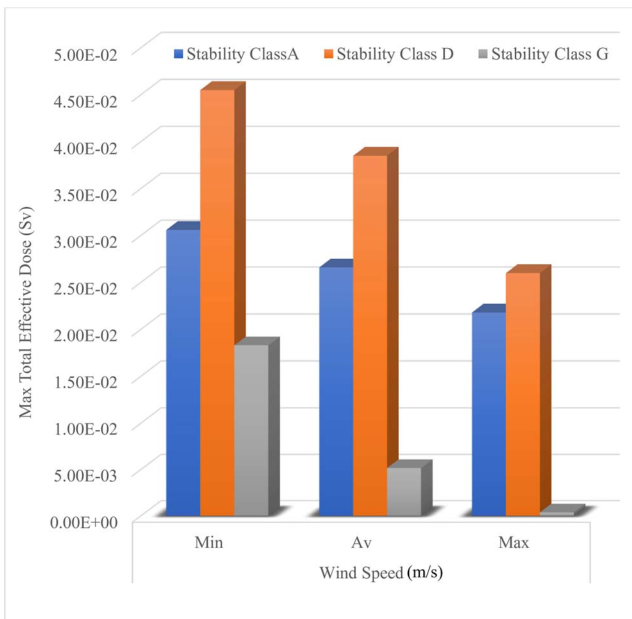

Figure 8. Variation of TEDE with wind speed in the dry season.

rapid response measures [25]. Stability class B encourages vertical and lateral dispersion due to moderate atmospheric turbulence. This leads to lower TEDE levels over a broader area as the plume disperses. During wet seasons, precipitation further aids in removing radionuclides from the air, reducing immediate exposure risks [27]. These findings highlight the need to adjust emergency response strategies based on specific atmospheric conditions and seasonal variations.

To assess how radionuclides spread and their potential effects, dose footprints for both the dry and wet seasons were created using the RASCAL 4.3.4 code, considering the stability classes B (slightly unstable) and D (neutral). These footprints help visualize how the radioactive plume behaves and the resulting TEDE. Figure 12 shows these dose footprints for the dry and wet seasons, specifically for the containment leakage release scenario. The simulations were performed under

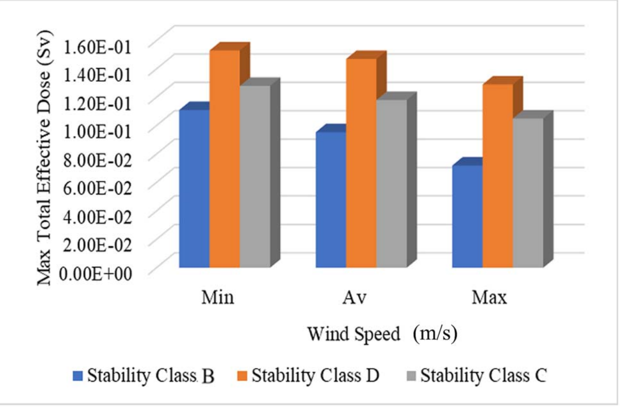

Figure 9. Variation of TEDE with wind speed in the wet season.

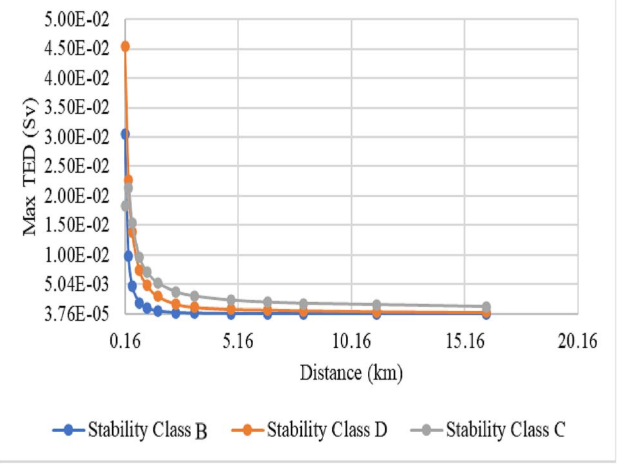

Figure 10. Variation of TEDE with distance from the release point—dry season.

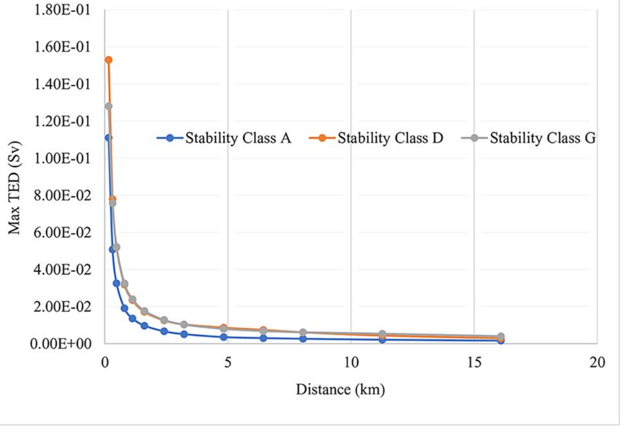

Figure 11. Variation of TEDE with distance from the release point—wet season.

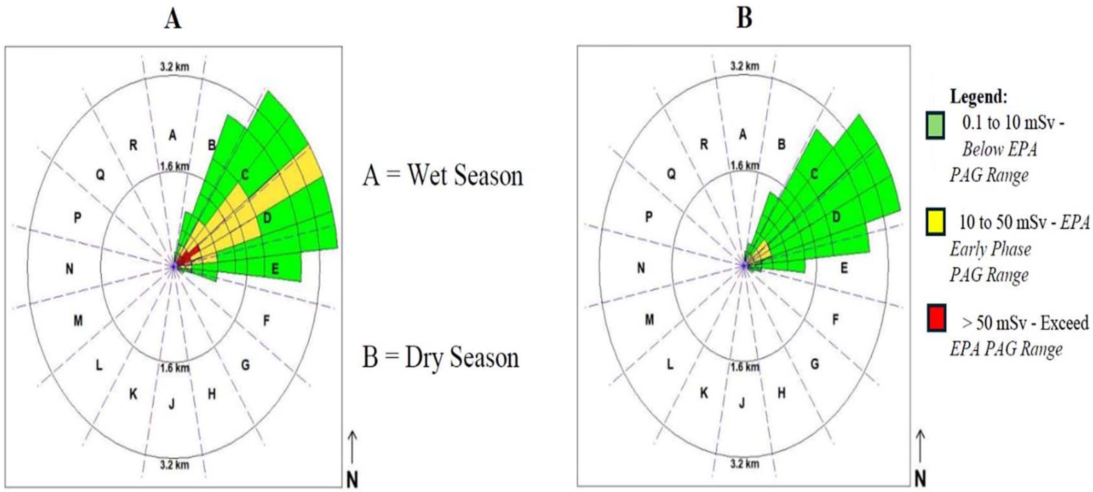

Figure 12. The dose footprint of TEDE shows the direction of released propagation in the wet and dry seasons.

conditions of minimal wind speed to ensure the highest possible deposition of the radionuclides.

Dose footprints are crucial for understanding how radiation spreads during a radiological release, as they depict variations in radiation exposure across different areas. High-risk zones are identified as areas where radiation exposure exceeds 50 mSv during the early phase, typically within the first few hours after a release. These zones demand immediate protective measures to reduce radiation exposure. Medium-risk zones are areas with exposure levels ranging from 10 to 50 mSv, this zone often overlaps with high-risk zones. In these areas, protective actions such as sheltering or limiting exposure may be required within the first 24–48 hours, depending on the specific circumstances. Low-risk zones, with exposure levels below 10 mSv, represent areas where protective actions are generally less likely to be necessary; however, continuous monitoring and assessment remain essential to ensure public safety. These classifications are consistent with the EPA's PAGs [24] and serve as a crucial framework for guiding protective measures during radiological emergencies.

These footprints also highlight seasonal differences (dry and wet seasons) in radionuclide dispersion, helping to design more effective safety measures. Overall, they play a key role in protecting public health, guiding regulatory decisions, and preparing for emergencies by showing the potential impact of radiation exposure. Figure 13 shows the external gamma exposure rate (mR/hour) as the sum of the cloudshine and groundshine dose rates corrected for the difference in energy absorption coefficients. In the dry season, the absence of rain allows ^{137}Cs and ^{133}Xe to stay in the atmosphere longer, resulting in extended exposure to radiation from their gamma emissions. Since there is no precipitation, groundshine exposure remains relatively low. However, without rainfall, these radioactive particles can spread more widely through the air, increasing the area of contamination. This creates a higher risk of inhaling ^{131}I and ^{133}Xe, especially in elevated areas where the spread of these particles is more intense.

Selected radionuclides

This study examines ^{137}Cs, ^{133}Xe, and ^{131}I, due to their varying health effects and changes in their release activities over time. Both ^{137}Cs and ^{131}I are beta emitters, which can lead to localized tissue damage if they are inhaled, ingested, or come into contact with the skin [13].

Figure 14 shows how the three radionuclides, ^{137}Cs, ^{133}Xe, and ^{131}I are released over time with ^{133}Xe, having the highest activity reflecting how easily it escapes. ^{131}I had a moderate release rate and ^{137}Cs released the least activity. The release rates of all three radionuclides stabilized when the core was recovered. ^{133}Xe released the highest activity as a noble gas but poses a lower health risk because it does not accumulate in body tissues and is less likely to cause direct tissue damage as compared to ^{137}Cs and ^{131}I. Table 6 reveals a notable difference in the ground concentration of radionuclide release amounts between the wet and dry seasons during containment leakage or failure scenarios.

In the wet season, approximately 1.35×10^{15} Bq of radionuclides were released, with noble gases making up the largest portion (70.5%), followed by iodine (22.7%). By contrast, the dry season showed a substantially higher release of 4.70×10^{18} Bq, consisting entirely of noble gases, with negligible detectable iodine or other radionuclides. The deposition of iodine was

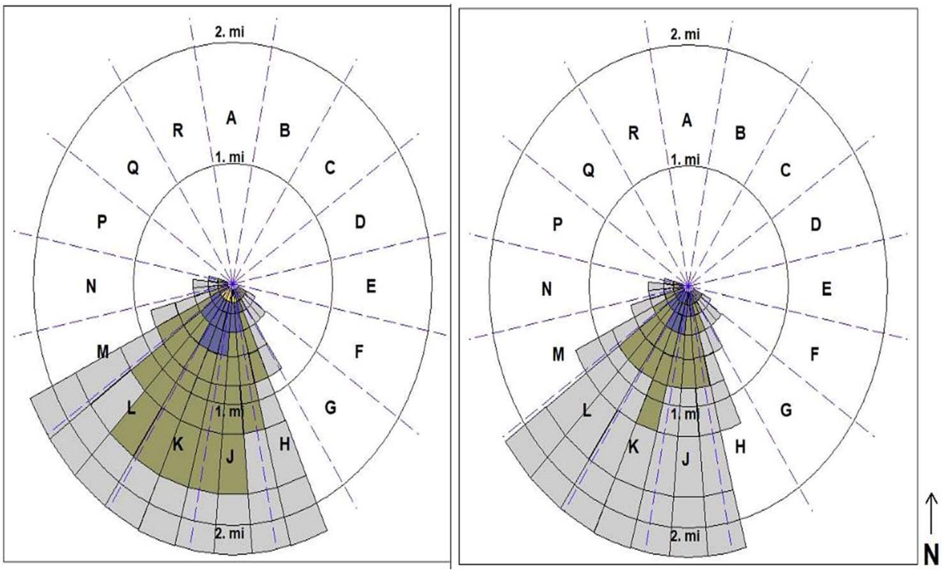

Figure 13. External gamma exposure rate from cloudshine and groundshine in the wet and dry seasons respectively.

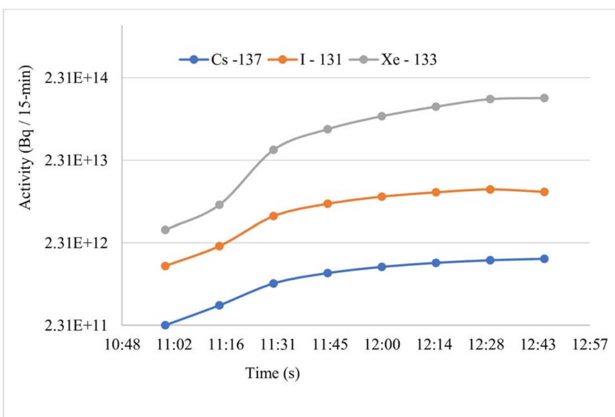

Figure 14. Release vs. time for containment leakage.

too negligible to have had any significant effect on the total activity released in the dry season. This difference aligns with similar studies, which suggest that dry conditions allow for greater airborne dispersion of noble gases due to the lack of moisture, which would otherwise aid in settling these particles out of the atmosphere [28]. The study also analyzed the ground concentrations of radionuclides such as ^{137}Cs and ^{131}I, while excluding ^{133}Xe due to its too-low concentration for detection by the code. The analysis was performed for dry and wet seasons under atmospheric stability classes B and D using simulations with minimum wind speeds to ensure maximum radionuclide deposition. The results showed that ground concentrations were higher during the wet season, likely due to rainfall, which aids in settling radionuclides. The highest total ground concentration for ^{137}Cs observed at 2.41 km from the release point was 6.22×10^3 kBq/m^2 in the dry season and 4.88×10^4 kBq/m^2 in the wet season. At the same distance, peak ground deposition concentrations of ^{131}I were 8.40×10^{-18} kBq/m^2 in the dry season and 3.07×10^3 kBq/m^2 in the wet season. These findings support previous studies, which suggest that wet conditions promote the deposition of radionuclides by aiding the settling of airborne particles [29, 30]. The results from Table 6 show that the ground concentration of radiation decreased moving farther away from the release source. This decrease happened because these substances spread out because of environmental factors such as wind and rain. This

Table 6. Ground concentration of radionuclides emission.

Distance (km)	Ground concentration of ^{137}Cs (kBq/m^2)		Ground concentration of ^{131}I (kBq/m^2)		Ground concentration—total (kBq/m^2)	
	Dry season	Wet season	Dry season	Wet season	Dry season	Wet season
0.16	1.67×10^1	1.85×10^1	1.77×10^{-18}	2.33×10^1	3.09×10^1	9.22×10^3
0.32	2.29×10^1	2.50×10^2	5.51×10^{-18}	5.14×10^1	6.03×10^2	4.74×10^4
0.48	5.07×10^1	3.72×10^2	8.07×10^{-18}	2.53×10^2	8.85×10^3	5.27×10^4
0.8	7.73×10^2	4.10×10^3	4.94×10^{-18}	7.36×10^2	9.97×10^4	8.09×10^4
1.13	8.78×10^2	5.33×10^3	6.46×10^{-18}	8.88×10^2	3.50×10^3	2.59×10^5
1.61	9.10×10^2	6.36×10^3	9.11×10^{-18}	9.48×10^2	5.97×10^3	5.21×10^5
2.41	6.22×10^3	4.88×10^4	8.40×10^{-18}	3.07×10^3	8.18×10^2	1.03×10^6
3.22	4.26×10^3	4.14×10^3	7.14×10^{-18}	2.10×10^2	9.44×10^2	7.46×10^5
4.83	3.04×10^2	3.51×10^3	5.99×10^{-19}	1.50×10^2	7.88×10^1	6.03×10^5
6.44	2.67×10^2	3.06×10^3	5.18×10^{-19}	1.32×10^2	4.10×10^1	4.90×10^4
8.05	2.27×10^1	2.57×10^3	4.33×10^{-19}	1.11×10^2	6.38×10^1	3.81×10^4
11.27	1.68×10^1	1.86×10^3	3.14×10^{-19}	8.18×10^1	4.52×10^0	2.66×10^3
16.09	1.15×10^1	1.26×10^3	2.11×10^{-19}	5.59×10^1	2.76×10^0	1.62×10^2

emphasizes the crucial role of both proximity and seasonal conditions in evaluating the potential exposure risks associated with radionuclide releases. The decline in concentration with distance is primarily due to environmental factors, such as wind and rainfall, which contribute to the dispersion of the radionuclides. A thorough understanding of these concentration levels is vital for accurately assessing the radiological effect on the environment.

Figure 15 shows how the ground concentration of radionuclides (^{137}Cs and ^{131}I) changes with distance from the source under the Dry and Wet season conditions. In wet conditions, radionuclide levels near the source are much higher, peaking at over 9×10^5 kBq/m^2, but drop steeply within the first few kilometers. On the other hand, dry conditions result in lower concentrations near the source, with a more gradual decrease over distance. Both scenarios indicate that the concentration drops quickly with distance, becoming negligible beyond 8 to 10 kilometers. Wet conditions, influenced by rainfall, cause radionuclides to settle closer to the source, creating more intense but localized contamination. Dry conditions, however, allow radionuclides to remain airborne longer, leading to a wider but less concentrated spread.

^{137}Cs, with its long half-life of 30 years, pose a long-term contamination threat, while ^{131}I, with its short 8-day half-life, is more of a concern in the early stages. These patterns highlight the need for targeted responses in wet conditions; cleanup efforts should focus on areas within 5 to 10 km of the release source, while in dry conditions, monitoring must cover a wider area. These values provide valuable information on the effectiveness of containment measures and help in planning for emergencies by identifying areas that may need more careful monitoring, evacuation and protection. By understanding the ground concentration effect, there is the likelihood of reducing exposure risks while improving preparedness for potential radiological events.

Protective actions based on TEDE and emergency preparedness strategy

Protective measures that rely on TEDE assessments are essential for protecting public health during radiological emergencies [31]. Examining the TEDE values can allow the creation of custom emergency preparedness strategies to effectively reduce radiation exposure. Effective nuclear emergency response plans prioritize evacuation, sheltering in place, and decontamination to safeguard public health by minimizing radiation exposure and associated risks. Based on United States EPA dose criteria, the recommended evacuation and sheltering distances were ∼2.0–4.1 km and 4.5–12 km in the dry season, and 2.3–4.6 km and 3.1–6.5 km in the wet season. In contrast, following the IAEA GSR Part 7 dose criteria, the evacuation and sheltering distances were determined to be 1.1–2.5 km and 2.5–4.25 km for the dry and wet seasons, respectively [29, 31]. Quick responses, especially in high-risk areas, are crucial for environmental protection. Monitoring TEDE levels also plays a vital role, offering real-time radiation data that guide adaptive protective actions. This approach is in line with recommendations from the International Commission on Radiological Protection (ICRP) for dynamic response strategies [32]. Additionally, incorporating Protective Action Guides (PAGs) that consider seasonal factors, like wet and

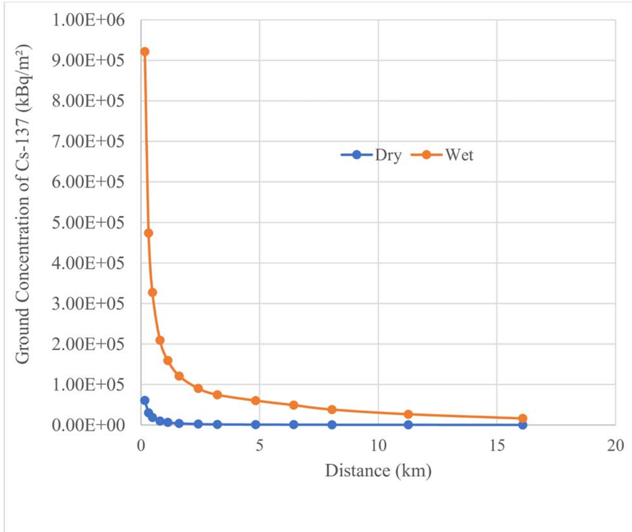

Figure 15. Total ground concentration of ^{137}Cs emissions for the wet and dry seasons.

Table 7. PAGs and protective actions for containment leakage during the wet season.

Site	Maximum dose (mSv) (distance [km])	PAG (mSv)	Impact area (km^2)	(Maximum distance [km]) dose (mSv)	Recommended protective action
(Prevailing Wind Direction = 240°)	33.12 (2.41)	50	0	(0.48) 52.0	Evacuation to 0.48 km
		10	0.1	(3.22) 10.4	Sheltering to 3.22 km
		0.1	3.8	(16.09) 2.93	Safe area from 3.22 km

dry conditions, further refines response effectiveness by addressing how seasonal variations impact radiological dispersion [33]. Tables 7 and 8 represent the PAGs and Protective Actions for containment leakage during the wet and dry seasons.

Based on information in Tables 7 and 8, to effectively tackle the potential radiological risks posed by containment leakage or failure, several emergency response strategies need to be implemented. Establishing a strong monitoring system is crucial to track radionuclide releases, particularly during the wet season when the ground concentration was 1.03×10^6 kBq/m^2 within 0.24 km of the release point. Monitoring environmental conditions is equally important to anticipate contaminant spread, and the research findings have contributed to the drafting of an EIA document which is currently under stakeholder review. Clear evacuation plans are vital, especially considering the significant release of 4.70×10^{18} Bq during the dry season, which consists entirely of noble gases. Regular drills conducted by emergency responders will equip them to be well-prepared for such emergencies. Public education campaigns are also necessary to raise awareness about the potential risks and the appropriate actions needed during a radiological emergency [34].

Radiological response plan

The qualitative analysis highlights the important roles played by the Ghana Atomic Energy Commission (GAEC), Nuclear Regulatory Authority (NRA), Ghana Health Service, and National Disaster Management Organization (NADMO) as presented in Table 9 through the nuclear security committee in Ghana's radiological emergency preparedness. Together, they have established a coordinated system that covers preparedness, communication, medical support, evacuation, and recovery, supported by trained healthcare workers and experts in decontamination. However, challenges such as limited funding, inadequate specialized resources, and low public awareness undermine their efforts and slow down recovery. Addressing these issues through increased funding, public education, and capacity building will strengthen collaboration among agencies and ensure a more effective response to nuclear emergencies.

Table 8. PAGs and protective actions for containment leakage during the dry season.

Site	Maximum dose (mSv) (distance [km])	PAG (mSv)	Impact area (km^2)	(Maximum distance [km]) dose (mSv)	Recommended protective action
(Prevailing Wind Direction = 240°)	27.11 (2.41)	50	0	NA	NA
		10	0	(0.48) 13.9	Sheltering to 0.48 km
		0.1	1.9	(16.09) 0.29	Safe area from 0.48 km

Table 9. Roles and response plans of key agencies.

Agency	Role in radiological accidents	Response plan
Ghana Nuclear Power Program Organization (GNPPO)	The unit will coordinate with agencies for nuclear emergencies.	Coordinates national response efforts and ensures communication between agencies.
Nuclear Regulatory Authority (NRA)	To ensure nuclear safety and regulatory compliance.	Monitors radiation levels, implements safety protocols and supervises risk mitigation efforts.
Nuclear Power Ghana (NPG)	The operator and owner of nuclear facilities are to implement safety protocols and emergency measures.	Implement emergency shut-down procedures where possible.
National Disaster Management Organization (NADMO)	In charge of coordinating disaster response and relief efforts, overseeing preparedness and strategies to reduce the impact of disasters.	Collaborate with GAEC, NRA, the Ministry of Health, and the Ghana Police Service and cover communication, medical support, decontamination, and recovery.

Conclusion

Assessing the radiological risks associated with possible containment leakage or failure at NPPs highlights the urgent need for effective emergency response strategies. The highest total ground concentration for ^{137}Cs observed at 2.41 km from the release point was 6.22 × 10^3 kBq/m^2 in the dry season and 4.88 × 10^4 kBq/m^2 in the wet season. At the same distance, peak ground deposition concentrations of ^{131}I were 8.40 × 10^{-18} kBq/m^2 in the dry season and 3.07 × 10^3 kBq/m^2 in the wet season. The significant variations in radionuclide releases between the wet and dry seasons, along with peak ground concentrations signal that immediate action is necessary. Essential strategies like strong monitoring systems, clear evacuation plans, and public education to reduce risks and safeguard public health are paramount. By focusing on protective measures informed by TEDE assessments, communities can strengthen their resilience against nuclear incidents, lower radiation exposure, and ensure the safety of residents living near nuclear facilities.

Acknowledgments

The authors thank the GAEC for information on the site and reactor type; and the Ghana Meteorological Agency for allowing the research team to use the site weather data.

Conflict of interest

None declared.

Funding

None declared.

References

1. IAEA. *Preparedness and Response for a Nuclear or Radiological Emergency (General Safety Requirements Part 7)*. International Atomic Energy Agency: Vienna, 2015.
2. EPA. *Protective Action Guides and Planning Guidance for Radiological Incidents*. U.S. Environmental Protection Agency: Washington, D.C., 2017.
3. Allotey NW, Ampomah-Amoako E, Enos E. *Nuclear Regulatory Authority Ghana Presentation, "No Need to Reinvent the Wheel", Panel Session for RIC 2004 Conference*, 2024.
4. Hasegawa A, Tanigawa K, Ohtsuru A. *et al.* Health effects of radiation and other health problems in the aftermath of nuclear accidents, with an emphasis on Fukushima. *Lancet* 2015;**386**:479–88. https://doi.org/10.1016/S0140-6736(15)61106-0
5. International Atomic Energy Agency IAEA. *The Chernobyl Accident: Updating of INSAG-1, Safety*. 1992.
6. International Atomic Energy Agency. *The Radiological Accident in Goiania*, IAEA, Vienna, 1988.

7. International Atomic Energy Agency. *Basic Safety Principles for Nuclear Power Plants 75-INSAG-3 Rev* 1 INSAG-12, 1999.
8. Sehgal BR. Severe accident management. In: *Nuclear Safety in Light Water Reactors*. Academic Press: Boston, 2012; 519–88.
9. Zhenying W, Yanming S, Huibo X. *et al*. Development of fuel product barrier monitoring system based on state functions in state-oriented emergency operating procedure. *Sci Technol Nucl Install* 2021;**2021**:1–9. https://doi.org/10.1155/2021/5596804
10. Ahn KI, Lee KH, Lee SW. *et al*. Estimation of fission product source terms for the SGTR accident of a reference PWR plant using MELCOR and MAAP5. *Nucl Eng Des* 2021;**371**:110967. https://doi.org/10.1016/j.nucengdes.2020.110967
11. International Atomic Energy Agency. *Safety Reports Series No. 52 Best Estimate Safety Analysis For Nuclear Power Plants: Uncertainty Evaluation*. 2008.
12. Reyes JN Jr, King JB Jr. Nuclear Engineering. *Encyclopedia of Energy*. Oregon State University Corvallis, Oregon, United States, Copyright © 2004 Elsevier Inc., 2004; **4**:315–31, 176480-X/00297-7. https://doi.org/10.1016/B0-12-176480-X/00297-7
13. Birikorang SA, Abrefah RG, Obeng HK. *et al*. Impact of strontium and krypton release from Ghana's MNSR following a conjectural accident scenario. *Sci Technol Nucl Install* 2019;**2019** Article ID 3026046:9. https://doi.org/doi.org/10.1155/2019/3026046
14. Gyamfi K, Birikorang SA, Ampomah-Amoako E. *et al*. Radiological safety analysis for a hypothetical accident of a generic VVER-1000 nuclear power plant. *Sci Technol Nucl Install* 2020;**2020** Article ID 4721971:8. https://doi.org/10.1155/2020/4721971
15. Obeng HK, Birikorang SA, Gyamfi K. *et al*. Assessment of radiological consequence of a hypothetical accident at the Ghana research Reactor-1 facility based on terrorist attack. *Sci Prog* 2021;**104**:1–24. https://doi.org/10.1177/00368504211054986
16. Usman B. "*Ghana Signs Deal with China for HPR1000 Nuclear Power Plant*", 2024.
17. Ramsdell JV, Athey GF, Rishe JP. RASCAL 4.3. RASCAL 4.3 WORKBOOK, Prepared for Office of Nuclear Regulatory Research U.S. Nuclear Regulatory Commission Washington, DC. 2013; 20555–0001.
18. *Series No. 75-INSAG-7, Vienna*. 1992.
19. Lucas DH, Moore DJ, Spurr G. The rise of hot plumes from chimneys. *Int J Air Water Poll* 1963;**7**:473–500.
20. Holland JZ. *A Meteorological Survey of the Oak Ridge Area*. USAEC Report 0110-99. Weather Bureau Office Oak Ridge, Tennessee, USA, 1953.
21. Stumke H. Vorschlaz einer empirischen Formel fur die Schornsteinuberhohung. *Stanb* 1963;**23**:549.
22. Amasy S, Ayman M, Atef M. CFD11-EG-4006 Air Quality Assessment of West Port-Said Industrial Region. *Proceedings of ICFD11: Eleventh International Conference of Fluid Dynamics*, Alexandria, Egypt, 2013.
23. San Joaquin Valley APCD. Guidance for Air Dispersion Modeling, USA, 2022.
24. Glyn R, Aiden P. Development and validation of loss of coolant accident (LOCA) simulation capability in the ENIGMA fuel performance code for zirconium-based cladding materials. *Nucl Eng Des* 2024;**416**:112767. https://doi.org/10.1016/j.nucengdes.2023.112767
25. Xiaole Z, Jing W. Atmospheric dispersion of chemical, biological, and radiological hazardous pollutants: informing risk assessment for public safety. *J Saf Sci Resilience* 2022;**3**:372–97.
26. Manual PAG. *Planning Guidance for Radiological Incidents EPA-400/R-17/001*, 2017.
27. Napier AB, Droppo JG, Rishel JP. *Air Dispersion Modeling of Radioactive Releases During Proposed PFP Complex Demolition Activities Report to CH2M*. HILL Plateau Remediation Company, Pacific Northwest National Laboratory Richland, Washington, USA, 2011.
28. International Atomic Energy Agency -TECDOC-760. *Modelling the Deposition of Airborne Radionuclides into the Urban Environment First Report of the VAMP Urban Working Group*. Part of the IAEA/CEC Coordinated Research Programme on the Validation of Environmental Model Predictions (VAMP), IAEA, Vienna, 1994.
29. International Atomic Energy Agency. *General Safety Requirements Part 7: Preparedness and Response for a Nuclear or Radiological Emergency*. IAEA: Vienna, 2015.
30. European Environment Agency; EEA Technical report No 10/2012; Particulate Matter from Natural Sources and Related Reporting under the EU Air Quality Directive in 2008 and 2009. European Environment Agency Kongens Nytorv Copenhagen, Denmark, 2012.
31. PAG Manual: Protective Action Guides and Planning Guidance for Radiological Incidents. PAG Manual Protective Action Guides and Planning Guidance for Radiological Incidents. Office of Radiation and Indoor Air Radiation Protection Division U.S. Environmental Protection Agency Washington, DC 20460, 2017.
32. International Atomic Energy Agency. *Preparedness and Response for a Nuclear or Radiological Emergency*. IAEA Safety Standards Series No. GSR Part 7. General Safety Requirements, IAEA, Vienna, 2015.
33. International Atomic Energy Agency. *Environmental and Source Monitoring for Purposes of Radiation Protection for Protecting People and the Environment No. RS-G-1.8 Safety Guide*, IAEA, Vienna, 2005.
34. International Commission on Radiological Protection (ICRP). *The 2007 Recommendations of the International Commission on Radiological Protection*. vol. **103**. ICRP Publication, Ltd., 2007.

Radiation Protection Dosimetry, 2025, 201, 333–350
https://doi.org/10.1093/rpd/ncaf024
Paper